

Constant Modulus and Reduced PAPR Block Differential Encoding for Frequency-Selective Channels

Yngvar Larsen, *Associate Member, IEEE*, Geert Leus, *Member, IEEE*, and Georgios B. Giannakis, *Fellow, IEEE*

Abstract—Frequency-selective channels can be converted to a set of flat-fading subchannels by employing orthogonal frequency-division multiplexing (OFDM). Conventional differential encoding on each subchannel, however, suffers from loss of multipath diversity, and a very high peak-to-average power ratio (PAPR), which causes undesirable nonlinear effects. To mitigate these effects, we design a block differential encoding scheme over the subchannels that preserves multipath diversity, and in addition, results in constant modulus transmitted symbols. This property is shown to ensure that the PAPR of the continuous-time transmitted waveform is reduced by a large factor. The maximum-likelihood decoder for the proposed scheme, conditioned on the current and previous received block, is shown to have linear complexity in the number of subcarriers. The constant modulus scheme will yield good bit-error rate performance with full rate only if short blocks are used. However, one may mitigate this problem by relaxing the constant modulus requirement. We show that in a practical OFDM system, we can group the subcarriers into shorter subblocks in a certain manner, and apply the constant modulus technique to each subblock. Thus, we improve diversity at a very low decoder complexity, and at the same time, we introduce an upper bound on the discrete-time PAPR, which, in turn, may lead to appreciable reduction in continuous-time PAPR, depending on the system parameters. Finally, in situations where we can sacrifice rate, additional complex field coding may be used to exploit the multipath diversity provided by channels longer than those the simple scheme can handle.

Index Terms—Block differential encoding, frequency-selective channels, orthogonal frequency-division multiplexing (OFDM), peak-to-average power ratio (PAPR).

Paper approved by C. Tellambura, the Editor for Modulation and Signal Design of the IEEE Communications Society. Manuscript received August 16, 2002; revised May 5, 2003 and August 16, 2003. The work of Y. Larsen was supported by the Research Council of Norway under Contract 134676/432. Prepared through collaborative participation in the Communications and Networks Consortium sponsored by the U.S. Army Research Laboratory under the Collaborative Technology Alliance Program, Cooperative Agreement DAAD19-01-2-0011. The U.S. Government is authorized to reproduce and distribute reprints for Government purposes notwithstanding any copyright notation thereon. This work was also supported by the National Science Foundation Wireless Initiative under Grant 99-79443. This paper was presented in part at the 36th Annual Conference on Information Sciences and Systems, Princeton, NJ, March 2002.

Y. Larsen was with the Department of Physics, University of Tromsø, NO-9037 Tromsø, Norway. He is now with NORUT Information Technology Ltd., NO-9294 Tromsø, Norway (e-mail: yngvar@itek.norut.no).

G. Leus is with the Faculty of Electrical Engineering, Mathematics, and Computer Science, Delft University of Technology, 2628 CD Delft, The Netherlands (e-mail: leus@cas.et.tudelft.nl).

G. B. Giannakis is with the Department of Electrical and Computer Engineering, University of Minnesota, Minneapolis, MN 55455 USA (e-mail: georgios@ece.umn.edu).

Digital Object Identifier 10.1109/TCOMM.2004.826413

I. INTRODUCTION

IN CASES WHERE it is undesirable or impossible to estimate the channel accurately at the receiver, one can rely on differential encoding schemes to eliminate the need for channel estimation at the receiver. Despite its importance, conventional differential encoding has been designed only for flat-fading channels, and exhibits an error floor when used with frequency-selective channels. Certainly, one can rely on orthogonal frequency-division multiplexing (OFDM) to transform a frequency-selective channel into a set of flat-fading subchannels; see, e.g., [13]. On each subchannel, one can then use the conventional differential encoding. Unfortunately, this technique suffers from loss of multipath diversity, and undesirable nonlinear effects due to very high peak-to-average power ratio (PAPR). A conventional way to exploit multipath diversity and reduce the PAPR is to employ coded differential OFDM (CDOFDM) [1], combined with a suitable PAPR reduction scheme, such as tone reservation [12].

In [7], a block differential encoding scheme over the subchannels that preserves the multipath diversity is designed. In this paper, we take a major step further, and design a block differential encoding scheme over the subchannels that not only preserves the multipath diversity, but also preserves the constant modulus property. The constant modulus transmitted symbols ensure that the PAPR remains low.

The proposed approach relies on constant modulus sequences that have ideal periodic autocorrelation properties, i.e., their autocorrelation functions are nonzero only for the zeroth lag [2], [9]. In order to design a differential encoding scheme that results in constant modulus transmissions, we will exploit the dual property: constant modulus sequences with ideal periodic autocorrelation properties have constant modulus entries also in the frequency domain.

Since the proposed constant modulus technique includes a form of repetition coding in the frequency domain with a rate that is inversely proportional to the square root of the number of subcarriers, we need to make up for the rate loss by using large size constellations. This implies that the block length can not be chosen arbitrarily large without losing either rate, or, bit-error rate (BER) performance. Thus, even common OFDM block lengths, like 64 or 128 symbols, may result in poor BER performance at full rate. However, if we relax the constant modulus requirement, it is possible to construct a system with low PAPR by grouping the subcarriers into shorter subblocks in a certain way, and apply the constant modulus scheme to each

subblock. This establishes an upper bound on the PAPR of the symbol-rate samples, which leads to an appreciable reduction of the continuous-time PAPR.

The rest of this paper is organized as follows. In Section II, we introduce the system model, and describe the concept of block differential encoding, in general. In Section III, we focus on the design of a block differential encoder that results in perfectly constant modulus transmissions. A low-complexity maximum-likelihood (ML) detector is introduced in Section IV, and its performance is analyzed in Section V. A subgrouping scheme that employs the constant modulus scheme on groups of subcarriers, with PAPR reduction as a result, is outlined in Section VI. In Section VII, we describe how additional complex field coding, linear in the phase domain, can enable extra multipath diversity, and thus improve performance, relative to the simple scheme in certain tradeoff situations. Finally, the methods are compared to existing schemes in Section VIII, and our main conclusions are summarized in Section IX.

Notation: Upper (lower) bold face letters are used for matrices (column vectors); $(\cdot)^T$ and $(\cdot)^H$ denote transpose and Hermitian transpose, respectively; $[\cdot]_{k,l}$ denotes the (k, l) th entry of a matrix, and $[\cdot]_k$ denotes the k th entry of a vector; \mathbf{I}_N denotes the $N \times N$ identity matrix; $\mathbf{0}_{M \times N}$ denotes an $M \times N$ all-zero matrix; $\mathbf{1}_{M \times N}$ denotes an $M \times N$ all-one matrix; $\text{diag}(\mathbf{x})$ is a diagonal matrix with the vector \mathbf{x} on its diagonal; $\text{tr}(\cdot)$ denotes matrix trace; $E(\cdot)$ denotes statistical average; and finally, the matrix defined by $[\mathbf{F}_N]_{k,l} \triangleq N^{-1/2} \exp(-j2\pi kl/N)$ is the $N \times N$ normalized fast Fourier transform (FFT) matrix.

II. SYSTEM DESCRIPTION

In transmissions over frequency-selective channels, channel-induced intersymbol interference (ISI) arises. To mitigate this dispersive effect, it has been proven useful to transmit and process the serial information symbols in blocks [13]. Specifically, the serial information symbols are grouped into $P \times 1$ blocks $\bar{\mathbf{u}}[i]$, where i is the block index, and the block length P is much larger than the channel order L . We define the $(L+1) \times 1$ channel tap vector by $\mathbf{h} \triangleq [h_0 \ \dots \ h_L]^T$, which throughout this paper is assumed to be zero-mean, multivariate complex Gaussian distributed. Define \mathbf{H}_0 as a $P \times P$ lower triangular Toeplitz matrix with the first column given by $[\mathbf{h}^T \ \mathbf{0}_{1 \times (P-L-1)}]^T$, and \mathbf{H}_1 as a $P \times P$ upper triangular Toeplitz matrix with the first row given by $[\mathbf{0}_{1 \times (P-L)} \ h_L \ h_{L-1} \ \dots \ h_1]$. We can now relate the received $P \times 1$ signal blocks $\bar{\mathbf{y}}[i]$ to the transmitted signal blocks $\bar{\mathbf{u}}[i]$ by [13]

$$\bar{\mathbf{y}}[i] = \mathbf{H}_0 \bar{\mathbf{u}}[i] + \mathbf{H}_1 \bar{\mathbf{u}}[i-1] + \bar{\mathbf{e}}[i] \quad (1)$$

where $\bar{\mathbf{e}}[i]$ denotes the $P \times 1$ noise block, which has independent and identically distributed (i.i.d.) zero-mean complex Gaussian entries with variance $\mathcal{N}_0/2$ per dimension.

The interblock interference (IBI), the second term in the right-hand side (RHS) of (1), can be removed by using a cyclic prefix of length \bar{L} , at the cost of reducing the spectral efficiency to $\eta = (P - \bar{L})/P$, where \bar{L} is an upper bound on the channel

order, which for the rest of this paper is assumed equal to the true channel order L , and available to both transmitter and receiver.

Now, replace the $P \times 1$ information block $\bar{\mathbf{u}}[i]$ in (1) by an $N \times 1$ information block $\mathbf{u}[i]$ preceded by a cyclic prefix of length L , such that $P = N + L$. At the receiver side, we discard the first L entries of the received $P \times 1$ vector $\bar{\mathbf{y}}[i]$ to obtain the $N \times 1$ vector $\mathbf{y}[i]$. The resulting $N \times N$ combined channel matrix \mathbf{H} is now circulant with $[\mathbf{h}^T \ \mathbf{0}_{1 \times (N-L-1)}]^T$ as its first column. This brings the input-output relationship to the matrix-vector form $\mathbf{y}[i] = \mathbf{H}\mathbf{u}[i] + \mathbf{e}[i]$, where the $N \times 1$ noise block $\mathbf{e}[i]$ consists of the last N entries of the original noise vector $\bar{\mathbf{e}}[i]$, see, e.g., [13].

Circulant matrices are diagonalized by FFT and inverse FFT (IFFT) operations. Thus, if we introduce the $N \times (L+1)$ matrix \mathbf{V} with $[\mathbf{V}]_{k,l} = \exp(-j2\pi kl/N)$, the circulant channel matrix can be factored as $\mathbf{H} = \mathbf{F}_N^H \mathbf{D}_H \mathbf{F}_N$, where $\mathbf{D}_H = \text{diag}(\mathbf{V}\mathbf{h})$ is a diagonal matrix with the N -point FFT of the channel tap vector \mathbf{h} along the diagonal. In order to convert the circulant channel matrix into a diagonal matrix, we start by letting each transmitted block $\mathbf{u}[i]$ be the IFFT of a block differentially encoded symbol block $\tilde{\mathbf{u}}[i]$; i.e., $\mathbf{u}[i] \triangleq \mathbf{F}_N^H \tilde{\mathbf{u}}[i]$. At the receiver, each block $\mathbf{y}[i]$ is FFT processed, leading to

$$\tilde{\mathbf{y}}[i] \triangleq \mathbf{F}_N \mathbf{y}[i] = \mathbf{D}_H \tilde{\mathbf{u}}[i] + \tilde{\mathbf{e}}[i] \quad (2)$$

where $\tilde{\mathbf{e}}[i] \triangleq \mathbf{F}_N \mathbf{e}[i]$. Observe that the system now consists of N flat-fading subchannels.

The block encoding process starts by defining a one-to-one map $\mathcal{M}(\cdot)$ from the set $\mathcal{A}_s^{RN \times 1}$ of $RN \times 1$ information-bearing symbol blocks $\mathbf{s}[i]$, to a group \mathcal{G} of $N \times N$ unitary and diagonal generator matrices $\mathbf{G}[i]$. Here, R is the code rate in information symbols per channel symbol. The generation of differentially encoded blocks follows the recursion

$$\tilde{\mathbf{u}}[i] = \begin{cases} \mathbf{G}[i] \tilde{\mathbf{u}}[i-1], & i > 0 \\ \tilde{\mathbf{u}}_0, & i = 0 \end{cases} \quad (3)$$

where the i th generator matrix $\mathbf{G}[i] \in \mathcal{G}$ conveys the information corresponding to the i th information symbol block $\mathbf{s}[i] \in \mathcal{A}_s^{RN \times 1}$.

Inserting (3) into (2), we obtain

$$\begin{aligned} \tilde{\mathbf{y}}[i] &= \mathbf{G}[i] \mathbf{D}_H \tilde{\mathbf{u}}[i-1] + \tilde{\mathbf{e}}[i] \\ \tilde{\mathbf{y}}[i-1] &= \mathbf{D}_H \tilde{\mathbf{u}}[i-1] + \tilde{\mathbf{e}}[i-1] \end{aligned} \quad (4)$$

where the diagonal matrices \mathbf{D}_H and $\mathbf{G}[i]$ commute. Hence, we find that successive received blocks obey the recursion

$$\tilde{\mathbf{y}}[i] = \mathbf{G}[i] \tilde{\mathbf{y}}[i-1] + \check{\mathbf{e}}[i] \quad (5)$$

where $\check{\mathbf{e}}[i] \triangleq \tilde{\mathbf{e}}[i] - \mathbf{G}[i] \tilde{\mathbf{e}}[i-1]$. Since both the FFT matrix and $\mathbf{G}[i]$ are unitary matrices, $\check{\mathbf{e}}[i]$ has entries that are i.i.d. zero-mean complex Gaussian variables with variance \mathcal{N}_0 per dimension. Note that this is twice the variance of the original noise vector $\mathbf{e}[i]$, which is a manifestation of the inherent 3-dB loss of differential detectors, relative to coherent detectors.

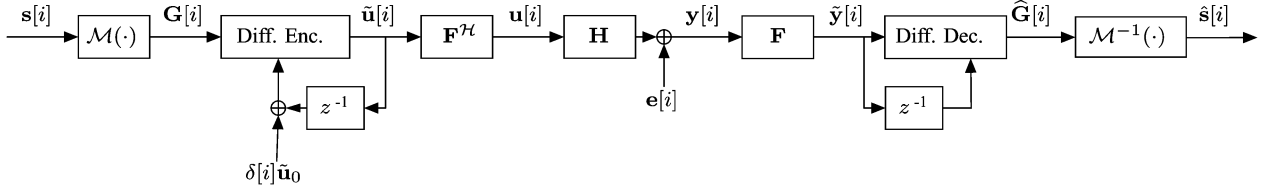


Fig. 1. Block diagram of the differential system described in Section II. The differential encoder is given in (3), and the differential decoder is given in (10). The n th original $N \times 1$ information block and the n th $N \times 1$ decoded block are denoted as $\mathbf{s}[i]$ and $\hat{\mathbf{s}}[i]$, respectively.

A block diagram of the block differential encoding system described in this section is shown in Fig. 1.

III. CONSTELLATION DESIGN

The main objective of this paper is to design $\tilde{\mathbf{u}}_0$ and \mathcal{G} such that the transmitted blocks $\mathbf{u}[i] = \mathbf{F}_N^H \tilde{\mathbf{u}}[i]$ have constant modulus entries. As $\tilde{\mathbf{u}}_0$, we choose one of the Zadoff–Chu sequences [2], [9]

$$[\tilde{\mathbf{u}}_0]_n \triangleq \begin{cases} \sqrt{E_s} \exp(j\frac{\pi}{N}n^2), & N \text{ even} \\ \sqrt{E_s} \exp[j\frac{\pi}{N}n(n+1)], & N \text{ odd} \end{cases} \quad (6)$$

where $n = 0, \dots, N-1$, and E_s is the energy of the transmitted symbols. This sequence has the remarkable property that $|\mathbf{F}_N \tilde{\mathbf{u}}_0|_n| = |\mathbf{F}_N^H \tilde{\mathbf{u}}_0|_n| = \sqrt{E_s}$, $\forall n$; i.e., the FFT and IFFT of the constant modulus $\tilde{\mathbf{u}}_0$ both retain constant modulus.

For a block length $N = K^2$, with $K \in \mathbb{N} = \{1, 2, 3, \dots\}$, we can define $N \times N$ generator matrices

$$\mathbf{G}_m = \mathbf{I}_K \otimes \text{diag}(\mathbf{g}_m), \quad m = 1, \dots, Q^{RN} \quad (7)$$

where $Q \triangleq |\mathcal{A}_s|$ is the cardinality of the alphabet of the input symbols, \otimes denotes the Kronecker product, and the entries of the $K \times 1$ information-bearing vector \mathbf{g}_m may be any unit modulus complex numbers. The \mathbf{g}_m can, for instance, be chosen from an alphabet $\mathcal{A}_g^{K \times 1}$ with cardinality $|\mathcal{A}_g^{K \times 1}| = |\mathcal{A}_s^{RN \times 1}| = Q^{RN}$. Thus, since the entries of \mathbf{g}_m must have unit modulus, we take them to be Q^{RK} -phase-shift keying (PSK) symbols.

The finite set $\mathcal{G} \triangleq \{\mathbf{G}_m\}_{m=1}^{Q^{RN}}$ now has the following important properties.

- P1)** All generator matrices $\mathbf{G}_m \in \mathcal{G}$ are diagonal and unitary.
- P2)** The set \mathcal{G} forms a group under matrix multiplication.
- P3)** The block vector $\mathbf{F}_N^H \mathbf{G}_m \tilde{\mathbf{u}}_0$ has constant modulus entries for all generator matrices $\mathbf{G}_m \in \mathcal{G}$ [9].

Notice that these properties ensure that all possible transmitted blocks have constant modulus entries.

IV. DETECTION

The ML detector, conditioned on $\tilde{\mathbf{y}}[i]$ and $\tilde{\mathbf{y}}[i-1]$, for the system described in Section III is given by

$$\hat{\mathbf{G}}[i] = \arg \min_{\mathbf{G} \in \mathcal{G}} \|\tilde{\mathbf{y}}[i] - \mathbf{G}\tilde{\mathbf{y}}[i-1]\|^2. \quad (8)$$

The complexity of this ML detector is exponential in the block length N . However, since the subchannels can be grouped into K groups that carry mutually independent information, it turns out that a major simplification is possible without losing the ML optimality. Define $\tilde{y}_{k,l} \triangleq [\tilde{\mathbf{y}}]_{k+lK}$, $g_k \triangleq [\mathbf{G}]_{k,k}$, and $\mathbf{g} \triangleq [g_0 \ g_1 \ \dots \ g_{K-1}]^T$. Then we can write (8) as

$$\begin{aligned} \hat{\mathbf{g}}[i] &= \arg \min_{\mathbf{g} \in \mathcal{A}_g^{K \times 1}} \left\{ \|\tilde{\mathbf{y}}[i]\|^2 + \|(\mathbf{I}_K \otimes \text{diag}(\mathbf{g}))\tilde{\mathbf{y}}[i-1]\|^2 \right. \\ &\quad \left. - 2\text{Re} \left\{ \tilde{\mathbf{y}}^H[i-1](\mathbf{I}_K \otimes \text{diag}(\mathbf{g}))^H \tilde{\mathbf{y}}[i] \right\} \right\} \\ &= \arg \max_{\mathbf{g} \in \mathcal{A}_g^{K \times 1}} \sum_{k=0}^{K-1} \text{Re} \left\{ g_k^* \sum_{l=0}^{K-1} \tilde{y}_{k,l}[i] \tilde{y}_{k,l}^*[i-1] \right\} \end{aligned} \quad (9)$$

where we have used that \mathbf{G} in (7) is unitary, and $g_k = g_{k+lK}$ for $k, l = 0, \dots, K-1$. Each of the terms in the outer summation can be maximized separately, since they correspond to mutually independent information. Recall that $\text{Re}\{z_1^* z_2\} = |z_1||z_2| \cos \theta$, where θ is the phase difference between the complex numbers z_1 and z_2 . Hence, $\text{Re}\{z_1^* z_2\}$ is maximized whenever the phase difference θ is minimized, and we can write

$$\hat{g}_k[i] = \exp\{j\theta_k[i]\}, \quad k = 0, \dots, K-1 \quad (10)$$

where $\theta_k[i]$ is the phase of $\sum_{l=0}^{K-1} \tilde{y}_{k,l}[i] \tilde{y}_{k,l}^*[i-1]$, the inner summation of (9), rounded to the closest multiple of $2\pi/Q^{RK}$. The complexity of this simplified ML decoder is linear in the block length N , which yields very efficient decoding.

The Kronecker product operation in (7) essentially corresponds to repetition coding over flat-fading subchannels in the frequency domain. Because an L th-order channel can have at most L zeros, one can argue that unique decodability of the system (5) in the absence of noise can be guaranteed if we choose $K = \sqrt{N} > L$; i.e., we repeat each information symbol more times than the maximum possible number of channel zeros. This can be confirmed also from (9). In the absence of noise, the inner sum is equal to the desired symbol $g_k[i]$, weighted by $\sum_{l=0}^{K-1} |[\mathbf{Vh}]_{k+lK}|^2$. This weight is real and positive $\forall \mathbf{h}$ if and only if $K > L$, since, in that case, not all the (nonnegative) terms can be zero. Hence, for the performance analysis in Section V, we will assume that $K \geq L+1$.

V. PERFORMANCE ANALYSIS

In this section, we will obtain high-signal-to-noise ratio (SNR) closed-form expressions for the diversity order and coding gain enabled by our block differential encoder. Based on these expressions, we will see that our scheme enables the

maximum possible multipath diversity order over (possibly correlated) frequency-selective channels.

The pairwise error probability (PEP) is defined as the probability that an ML detector incorrectly decodes an information block $\mathbf{s}[i]$ as $\mathbf{s}'[i]$. Under the assumptions that the channel vector is multivariate zero-mean complex Gaussian distributed, and the SNR is high, the conditional PEP is upper bounded by [11]

$$P(\mathbf{s} \rightarrow \mathbf{s}' | \hat{\mathbf{y}}[i-1]) \leq \exp \left[\frac{d^2(\mathbf{G}, \mathbf{G}') E_s}{8\mathcal{N}_0} \right] \quad (11)$$

where $d^2(\mathbf{G}, \mathbf{G}') \triangleq E_s^{-1} \|(\mathbf{G} - \mathbf{G}') \hat{\mathbf{y}}[i-1]\|^2$. We have dropped the block indexes of the information blocks \mathbf{s} and \mathbf{s}' , and generator matrices \mathbf{G} and \mathbf{G}' for notational convenience. At high SNR, we can ignore the terms of $d^2(\mathbf{G}, \mathbf{G}')$ that depend on $\hat{\mathbf{y}}[i-1]$. This means that $\hat{\mathbf{y}}[i-1] \approx \mathbf{D}_H \hat{\mathbf{u}}[i-1] = \mathbf{D}_u \mathbf{V} \mathbf{h}$, with $\mathbf{D}_u \triangleq \text{diag}\{\hat{\mathbf{u}}[i-1]\}$, such that we can write the Euclidean distance $d^2(\mathbf{G}, \mathbf{G}')$ as $d^2(\mathbf{G}, \mathbf{G}') = E_s^{-1} \|(\mathbf{G} - \mathbf{G}') \mathbf{D}_u \mathbf{V} \mathbf{h}\|^2 = E_s^{-1} \mathbf{h}^H \mathbf{V}^H \mathbf{D}_u^H \mathbf{D}_g^2 \mathbf{D}_u \mathbf{V} \mathbf{h} = \mathbf{h}^H \mathbf{V}^H \mathbf{D}_g^2 \mathbf{V} \mathbf{h}$, where $\mathbf{D}_g^2 \triangleq (\mathbf{G} - \mathbf{G}')^H (\mathbf{G} - \mathbf{G}')$. Note that since $E_s^{-1} \mathbf{D}_u^H \mathbf{D}_u = \mathbf{I}_N$, $d^2(\mathbf{G}, \mathbf{G}')$ is independent of the previous transmitted symbol $\hat{\mathbf{u}}[i-1]$.

In general, the entries of the $(L+1) \times 1$ channel vector \mathbf{h} are correlated, with correlation matrix $\mathbf{R}_h \triangleq E\{\mathbf{h}\mathbf{h}^H\}$. The rank of this matrix satisfies $r_h \triangleq \text{rank}(\mathbf{R}_h) \leq L+1$. Eigenvalue decomposition of \mathbf{R}_h yields

$$\mathbf{R}_h = \mathbf{U}_h \mathbf{\Sigma}_h \mathbf{U}_h^H \quad (12)$$

where $\mathbf{\Sigma}_h \triangleq \text{diag}\{\sigma_0^2, \sigma_1^2, \dots, \sigma_{r_h-1}^2\}$ is an $r_h \times r_h$ positive definite diagonal matrix with the nonzero eigenvalues along the diagonal, and \mathbf{U}_h is an $(L+1) \times r_h$ matrix with the corresponding orthonormal eigenvectors as columns. Now, define the $r_h \times 1$ prewhitened channel vector $\bar{\mathbf{h}} \triangleq \mathbf{\Sigma}_h^{-1/2} \mathbf{U}_h^H \mathbf{h} \triangleq [\bar{h}_0, \bar{h}_1, \dots, \bar{h}_{r_h-1}]^T$, with correlation matrix given by $\mathbf{R}_{\bar{h}} = E\{\bar{\mathbf{h}}\bar{\mathbf{h}}^H\} = \mathbf{I}_{r_h}$. Then we can write

$$d^2(\mathbf{G}, \mathbf{G}') = \bar{\mathbf{h}}^H \mathbf{A}_e \bar{\mathbf{h}} \quad (13)$$

where $\mathbf{A}_e \triangleq \mathbf{\Sigma}_h^{1/2} \mathbf{U}_h^H \tilde{\mathbf{A}}_e \mathbf{U}_h \mathbf{\Sigma}_h^{1/2}$, and $\tilde{\mathbf{A}}_e \triangleq \mathbf{V}^H \mathbf{D}_g^2 \mathbf{V}$. To further simplify this equation, we start by dividing the matrix \mathbf{V} into $K \times (L+1)$ submatrices $\tilde{\mathbf{V}}_p$, where $[\tilde{\mathbf{V}}_p]_{k,l} \triangleq [\mathbf{V}]_{k, K+p, l} = \exp(-j2\pi p/N) \exp(-j2\pi kl/K)$, $p = 0, \dots, K-1$, such that we have $\tilde{\mathbf{V}}_p = \exp(-j2\pi p/N) \tilde{\mathbf{V}}_0$. Observe that $\tilde{\mathbf{V}}_p^H \tilde{\mathbf{V}}_p = K \mathbf{I}_{L+1}$, $\forall p$ if $K \geq L+1$, which is already assumed in order to guarantee unique decodability. If we then define the $K \times 1$ error vector \mathbf{g}_e as the difference $\mathbf{g}_e \triangleq \mathbf{g} - \mathbf{g}'$ between the information vectors corresponding to \mathbf{G} and \mathbf{G}' , respectively [cf. (7)], we can write

$$\tilde{\mathbf{A}}_e = \sum_{p=0}^{K-1} \|\mathbf{g}_e\|_p^2 \tilde{\mathbf{V}}_p^H \tilde{\mathbf{V}}_p = K \|\mathbf{g}_e\|^2 \mathbf{I}_{L+1} \quad (14)$$

which shows that (13) can be written as

$$d^2(\mathbf{G}, \mathbf{G}') = K \|\mathbf{g}_e\|^2 \bar{\mathbf{h}}^H \mathbf{\Sigma}_h \bar{\mathbf{h}} = K \|\mathbf{g}_e\|^2 \sum_{l=0}^{r_h-1} \sigma_l^2 |\bar{h}_l|^2. \quad (15)$$

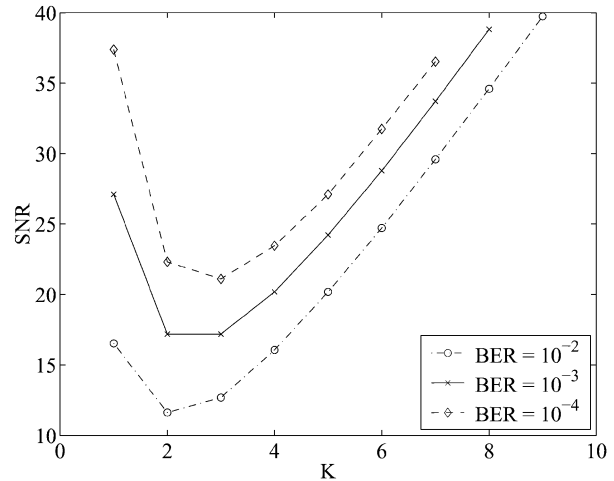


Fig. 2. Required SNR versus K for systems with rate $R \log_2 Q = 1$, and given values of BER.

Inserting (15) into (11), and averaging with respect to the i.i.d. Rayleigh random variables $|\bar{h}_l|^2$ gives us an upper bound on the average PEP at high SNR (see also [11])

$$\begin{aligned} P(\mathbf{s} \rightarrow \mathbf{s}') &\leq \prod_{l=0}^{r_h-1} \left(1 + \frac{1}{2} K \|\mathbf{g}_e\|^2 \sigma_l^2 \frac{E_s}{4\mathcal{N}_0} \right)^{-1} \\ &\leq \left(\frac{E_s}{4\mathcal{N}_0} \right)^{-r_h} \left(\prod_{l=0}^{r_h-1} \frac{1}{2} K \|\mathbf{g}_e\|^2 \sigma_l^2 \right)^{-1} \\ &\triangleq \left(\frac{G_{c,e} E_s}{4\mathcal{N}_0} \right)^{-G_{d,e}}. \end{aligned} \quad (16)$$

The diversity order G_d is defined as $\min_{\mathbf{g}_e \neq \mathbf{0}} G_{d,e}$, i.e., the slope of the average PEP as a function of SNR, on a doubly logarithmic scale, minimized over all possible error vectors \mathbf{g}_e . This slope is, in general, determined by the rank of the matrix $\tilde{\mathbf{A}}_e$. If $\tilde{\mathbf{A}}_e$ has full rank $\forall \mathbf{g}_e \neq \mathbf{0}$, the diversity order is

$$G_d^{\max} = \text{rank}(\mathbf{R}_h) = r_h \leq L+1 \quad (17)$$

which is the maximum achievable for a given channel. In our case, (14) shows that $\tilde{\mathbf{A}}_e$ has full rank $\forall \mathbf{g}_e \neq \mathbf{0}$, which implies that maximum diversity is achieved by our method.

The coding gain G_c is defined as

$$\begin{aligned} G_c &\triangleq \min_{\mathbf{g}_e \neq \mathbf{0}} G_{c,e} = \min_{\mathbf{g}_e \neq \mathbf{0}} \frac{1}{2} K \|\mathbf{g}_e\|^2 \left(\prod_{l=0}^{r_h-1} \sigma_l^2 \right)^{1/r_h} \\ &= \frac{1}{2} K d_{\min}^2 \det^{1/r_h}(\mathbf{\Sigma}_h) \end{aligned} \quad (18)$$

where $d_{\min}^2 \triangleq \min_{\mathbf{g}_e \neq \mathbf{0}} \|\mathbf{g}_e\|^2 = 4 \sin^2(\pi/Q^{RK})$ is the minimum distance between two symbols in a Q^{RK} -PSK constellation. Despite the linear factor K , the exponential decrease of d_{\min} with K causes the coding gain to decrease monotonically with K . Fig. 2 shows the SNR needed to achieve a given BER as a function of K , estimated from Monte Carlo simulations. We have used a rate of $R \log_2 Q = 1$. Due to the requirement that $K > L$, we cannot use the same channel for each value of K (unless $L = 0$, which is uninteresting). Thus, we choose $K = L+1$, which enables the maximum possible multipath diversity for each K . The results also hold for cases where

$N > L > K - 1$, i.e., if we do not exploit all multipath diversity provided by the channel. Note that including the cyclic prefix overhead, the overall rate is now, in fact, a slowly varying function of K given by $N/(N + L) = 1/(1 + 1/K - 1/K^2)$ b/s/Hz. We observe that for $K \geq 4$, the required SNR to achieve a given BER starts to increase exponentially. Thus, $K = 4$ may be the largest acceptable value in a practical situation, which limits the maximum block length to $N = 16$. In Section VI, we will propose a subchannel grouping scheme, where each subchannel group may contain only $N = K^2 \leq 16$ elements. This will improve BER performance at the cost of higher PAPR than the proposed constant modulus scheme.

The factor $1/2$ in (18) reflects the 3-dB loss, compared with a coherent receiver. By employing multiple-symbol differential detection [4], this 3-dB loss can be partially recovered, at the cost of increased decoding complexity and delay. This method exploits the fact that a differentially encoded system has infinite memory under time-invariant channel conditions. Analysis of such a system, however, is beyond the scope of this paper.

VI. PAPR REDUCTION BY SUBCHANNEL GROUPING

Recall that the coding gain in (18) is a monotonically decreasing function of K for fixed Q and R . This is due to the need for a higher order PSK constellation to make up for the rate loss caused by the inherent repetition coding, cf. (7). In an OFDM context where the channel, and thus the required block length, may be long, this is an obvious drawback. For instance, in a system with $N = 64 = 8^2$ subcarriers, we need to use Q^{8R} -PSK symbols. To maintain a reasonable rate, say $R = 3/4$ with binary (B)PSK signaling ($Q = 2$), this amounts to using 64-PSK symbols, which, in turn, leads to unacceptable performance, in spite of the eight-fold repetition code. In fact, it has been noted in related contexts that in order to keep the discrete-time PAPR under a specified threshold when the block length increases, one has to sacrifice either rate or minimum Euclidean distance in the constellation [8]. Thus, perfect constant modulus transmitted symbols in a *differential* OFDM system may not always be practical (though in the coherent case, one can, for instance, achieve this by using single-carrier block transmissions as suggested in [15]). However, we may relax the constant modulus requirement. Keeping the PAPR of symbol-rate samples below a specified level may be sufficient for practical purposes, and that is the approach we will follow in this section.

Let the $P \times 1$ transmitted block $\tilde{\mathbf{u}}[i]$ be the $\tilde{N} \times 1$ block $\mathbf{u}[i] \triangleq \mathbf{F}_{\tilde{N}}^H \tilde{\mathbf{u}}[i]$, with a cyclic prefix of length $L = P - \tilde{N}$ inserted. Let also the block length of the OFDM system be $\tilde{N} = MN$, where $N = K^2$ as in Section V, and M is the number of partitions. The discrete-time PAPR is now defined as

$$\text{PAPR} \triangleq \frac{\max_i \|\tilde{\mathbf{u}}[i]\|_\infty^2}{E\{\|\tilde{\mathbf{u}}[i]\|_\infty^2\}}/P \quad (19)$$

where we have assumed ∞ -norm ergodicity of the ensemble $\{\tilde{\mathbf{u}}[i]\}$, i.e., we have transmitted enough blocks for $\|\tilde{\mathbf{u}}[i]\|_\infty^2$ to reach its maximum value for some i . This is equivalent to the true PAPR, when rectangular shaping pulses are assumed. For realistic shaping pulses, one has to consider the PAPR of an

oversampled and filtered version of the symbol block $\tilde{\mathbf{u}}[i]$, defined as in (19), but with $\tilde{\mathbf{u}}[i]$ replaced by the oversampled and filtered version. In the simulations, we will take this into account. However, the analysis below will use the definition in (19), assuming that reduction of the PAPR of the critically sampled signal will lead to a PAPR reduction also for the continuous-time waveform.

For any OFDM with PSK symbols, we have $E\{\|\tilde{\mathbf{u}}[i]\|_\infty^2\} = (P/\tilde{N})E\{\|\mathbf{F}_{\tilde{N}}^H \tilde{\mathbf{u}}[i]\|_\infty^2\} = (P/\tilde{N})E\{\|\tilde{\mathbf{u}}[i]\|_\infty^2\} = PE_s$. Also, we have $\|\tilde{\mathbf{u}}[i]\|_\infty^2 = \|\mathbf{F}_{\tilde{N}}^H \tilde{\mathbf{u}}[i]\|_\infty^2 \leq \tilde{N}E_s$, with equality if $\tilde{\mathbf{u}}[i] = u\mathbf{1}_{\tilde{N} \times 1}$, where u is any PSK symbol. Substituting these into (19), we find that $\text{PAPR} = \tilde{N}$.

Note that since the channel order L could be relatively large, we may not choose $K \geq L + 1$, such that we do not enable maximum diversity anymore. However, a diversity order of, for instance, $K = 4$ may be sufficient, since the scheme must be combined with some kind of error-control coding in practice.

Let the index set of the \tilde{N} subchannels be denoted by $\mathcal{I} = \{0, 1, \dots, \tilde{N} - 1\}$. Following the idea in [3], [5], and [13], we can now represent the subchannel grouping by partitioning \mathcal{I} into M nonintersecting index subsets of equal size N given by

$$\begin{aligned} \mathcal{I}_\mu &= \{\mu, M + \mu, \dots, (N - 1)M + \mu\} \\ \mu &= 0, \dots, M - 1. \end{aligned} \quad (20)$$

In the following, we will drop the block index i for notational convenience. Now, let $\tilde{\mathbf{u}}_\mu$ be the $N \times 1$ subblock of the $\tilde{N} \times 1$ information block $\tilde{\mathbf{u}}$ corresponding to the index subset \mathcal{I}_μ , and define the $\tilde{N} \times \tilde{N}$ diagonal matrix $\mathcal{D} \triangleq \text{diag}([1 \ \exp(j(2\pi/\tilde{N})) \ \dots \ \exp(j(2\pi(\tilde{N} - 1)/\tilde{N}))])$. Then the transmitted symbol block can be written as

$$\mathbf{F}_{\tilde{N}}^H \tilde{\mathbf{u}} = \frac{1}{\sqrt{M}} \sum_{\mu=0}^{M-1} \mathcal{D}^\mu (\mathbf{1}_{M \times 1} \otimes \mathbf{F}_N^H \tilde{\mathbf{u}}_\mu). \quad (21)$$

By applying the constant modulus block differential encoding described in Section III on the subblocks $\tilde{\mathbf{u}}_\mu$ separately, we obtain

$$\begin{aligned} \|\mathbf{F}_{\tilde{N}}^H \tilde{\mathbf{u}}\|_\infty^2 &= \frac{1}{M} \left\| \sum_{\mu=0}^{M-1} \mathcal{D}^\mu (\mathbf{1}_{M \times 1} \otimes \mathbf{F}_N^H \tilde{\mathbf{u}}_\mu) \right\|_\infty^2 \\ &\leq \frac{E_s}{M} \left\| \sum_{\mu=0}^{M-1} \mathbf{1}_{\tilde{N} \times 1} \right\|_\infty^2 = ME_s \end{aligned} \quad (22)$$

where we have used that $\|\mathbf{F}_N^H \tilde{\mathbf{u}}_\mu\|_\infty^2 = E_s, \forall \mu$ by design, which means that each entry per subblock has a maximum modulus of $\sqrt{E_s}$. The maximum ∞ -norm is attained, for instance, if $\tilde{\mathbf{u}} = \mathbf{1}_{\tilde{N} \times 1}$. The discrete-time PAPR can now be expressed as $\text{PAPR} = (ME_s)/(PE_s/P) = M$. This amounts to a reduction of the discrete-time PAPR by a factor of $\tilde{N}/M = N$ relative to the conventional OFDM system. This will lead to a reduction of the continuous-time PAPR. The resulting reduction of nonlinear effects will be good to moderate depending on the system parameters, as will be shown in Section VIII.

VII. COMPLEX-FIELD CODING

In Section VI, we have mapped groups of $b = RK \log_2(Q)$ information bits to each Q^{RK} -PSK entry in the vector $\mathbf{g}[i]$ by, for instance, a Gray mapping. This enables the simplified ML

decoder in (10). Letting $\exp(\cdot)$ denote entrywise exponentiation, we can write this as

$$\mathbf{g}[i] = \mathcal{M}(\mathbf{b}[i]) = \exp \left\{ \frac{j2\pi}{Q^{RK}} (\mathbf{I}_K \otimes \mathcal{M}_G) \mathbf{b}[i] \right\} \quad (23)$$

where $\mathbf{b}[i]$ is a $Kb \times 1$ bit vector formed by stacking the bits corresponding to the symbols in the $RK \times 1$ input block $\mathbf{s}[i]$, and \mathcal{M}_G is a Gray mapping from a $b \times 1$ bit vector to the corresponding PSK waveform number. (Note that this is a slight abuse of the Kronecker notation, since the mapping \mathcal{M}_G is not strictly linear.) The Gray mapping \mathcal{M}_G can be implemented as

$$\begin{aligned} \mathcal{M}_G(\mathbf{x}) &= [2^{b-1} \ \dots \ 2 \ 1] \left(\mathbf{x} \oplus \left\lfloor \frac{\mathbf{x}}{2} \right\rfloor \right) \\ &= [2^{b-1} \ \dots \ 2 \ 1] (\mathbf{M}_G \mathbf{x} \bmod 2) \end{aligned} \quad (24)$$

where \oplus denotes modulo 2 addition, \mathbf{x} is a $b \times 1$ bit vector, and the $b \times b$ matrix \mathbf{M}_G is defined by

$$\mathbf{M}_G \triangleq \begin{bmatrix} 1 & 1 & 0 & \dots & 0 & 0 \\ 0 & 1 & 1 & & 0 & 0 \\ \vdots & & & \ddots & & \vdots \\ 0 & \dots & 0 & 1 & 1 \\ 0 & 0 & \dots & 0 & 1 \end{bmatrix}. \quad (25)$$

When $K < L + 1$, this system does not enable maximum diversity. Thus, by additional coding, we may enable the maximum possible diversity in (17). A bandwidth-efficient means of enabling extra diversity is by complex field coding over the different elements in $\mathbf{g}[i]$, at the cost of increased receiver complexity. Since the elements of $\mathbf{g}[i]$ still need to have unit modulus, we may only perform transformations in the phase domain. Toward this end, we define a new mapping

$$\begin{aligned} \mathcal{M}(\mathbf{b}[i]) &= \exp \left\{ \frac{j2\pi}{Q^{RK}} \boldsymbol{\Theta} (\mathbf{I}_K \otimes \mathcal{M}_G) \mathbf{b}[i] \right\} \\ &= \exp \left\{ \frac{j2\pi}{Q^{RK}} (\boldsymbol{\Theta} \otimes \mathcal{M}_G) \mathbf{b}[i] \right\} \end{aligned} \quad (26)$$

where $\boldsymbol{\Theta}$ is a $K \times K$ matrix. The design of the coding matrix $\boldsymbol{\Theta}$ is somewhat different from the coding matrices in, e.g., [14], in that they operate in the (modular) phase space. This implies that $\boldsymbol{\Theta}$ has to be real, and that the sum of the entries of the vector $(\boldsymbol{\Theta} \otimes \mathcal{M}_G) \mathbf{b}[i]$ need to be bounded to avoid phase wrapping. In addition, the sum of the elements of any row in $\boldsymbol{\Theta}$ must be strictly less than $Q^{RK}/(Q^{RK} - 1)$, and all elements must be nonnegative. One way to construct such a matrix $\boldsymbol{\Theta}$ is to let it be a circulant matrix with $[1 \ Q^{-RK} \ \dots \ Q^{-RK(K-1)}]$ as its first row. Using such a $\boldsymbol{\Theta}$ will enable us to recover the vector $\mathbf{b}[i]$ from a single entry of $\mathcal{M}(\mathbf{b}[i])$, since it corresponds to mapping the Kb bits in the vector $\mathbf{b}[i]$ to a Q^{RN} -PSK constellation in K different ways. Following steps similar to those in [14], it can be shown that such a $\boldsymbol{\Theta}$ will ensure the maximum possible diversity order r_h , even when $K < L + 1$.

The design in the previous paragraph will work, but since the rightmost elements of the first row of $\boldsymbol{\Theta}$ are very small (or equivalently, the resulting constellation has a very large dimension), the diversity enabled by the complex field coding will show up only at very high SNR. In practice, only the two largest elements will contribute to the performance for realistic SNR

values. Therefore, we may choose $\boldsymbol{\Theta}$ to be a circulant matrix with $[1 \ Q^{-RK} \ 0 \ \dots \ 0]$ as its first row. Note that Q^{-RK} may be a very small number if RK is large. The size of this number obviously determines the level of SNR for which the extra diversity starts to show up. Thus, we may conclude that for given values of Q and K , the complex field coding discussed in this section may only be worthwhile for small values of R . In practice, this means that for full-rate systems ($R = 1$), complex field coding will not improve performance for practical SNR values. In Section VIII-D, we demonstrate this effect by numerical simulations.

VIII. NUMERICAL SIMULATIONS

In this section, we will demonstrate the performance of the methods developed in this paper by numerical simulations.

A. Comparison With Conventional Differential Encoding

To demonstrate the capability of the constant modulus scheme in a single-carrier context, we consider signaling over a two-path channel. Such a channel could, in a practical situation, arise as the result of an inaccurate blind channel equalization procedure. The 2×1 channel tap vector $\mathbf{h} \triangleq [h_0 \ h_1]^T$ is zero-mean complex Gaussian, with covariance matrix $\mathbf{R}_h = \text{diag}\{\sigma_0^2 \ \sigma_1^2\}$. To ensure unique decodability, we choose $K = L + 1 = 2$, which yields a block length $N = K^2 = 4$. The spectral efficiency is $\eta = 4/(4 + 1) = 0.8$. We consider BPSK information symbols ($Q = 2$) and rate $R = 1$, such that $|\mathcal{A}_g| = Q^{RK} = 4$. Thus, the entries of \mathbf{g}_m in (7) must be chosen from a quaternary (Q)PSK constellation. To increase the coding gain of our system, we let the map $\mathcal{M}(\cdot)$ be a Gray mapping, e.g., [10, p. 170].

We will compare the performance of our proposed transmission scheme with that of conventional differential BPSK (DBPSK); see, e.g., [10, p. 272]. Due to the nonflat channel response, the DBPSK scheme will suffer from ISI, which will result in saturation of the BER curve. We will consider two different channels: **Ch1**): $\sigma_0^2 = 2/3$ and $\sigma_1^2 = 1/3$; and **Ch2**): $\sigma_0^2 = 1/1.05$ and $\sigma_1^2 = 0.05/1.05$.

For our proposed scheme, we will use the ML detector in (10), while for the DBPSK scheme, we will use the detector given by $\hat{s}[i] = \arg \min_{s \in \{-1, 1\}} \|y[i] - sy[i-1]\|^2$, where $y[i]$ and $\hat{s}[i]$ denote the received samples and the detected symbols, respectively. This detector is ML optimal in the flat-fading case. Hence, it is natural to compare the performance of our method with this.

Fig. 3 shows BER as a function of SNR, where we have defined $\text{SNR} = E\|\mathbf{H}\mathbf{u}\|^2/E\|\mathbf{e}\|^2 = \text{tr}(\mathbf{R}_h)E_s/\mathcal{N}_0$. In the first channel, we have significant ISI, and as expected, the performance of the conventional DBPSK scheme is poor. Our scheme, on the other hand, exploits the diversity provided by the multipath channel, as seen by the slope of the BER curve. Channel **Ch2**) is very close to flat fading, since the second channel path has much lower power than the first. Nevertheless, a significant error floor is present in the DBPSK curve. The constant modulus scheme, on the other hand, exploits the multipath diversity, but the coding gain decreases compared with the first example, due to the reduced $\det(\mathbf{R}_h)$ [cf. (18)].

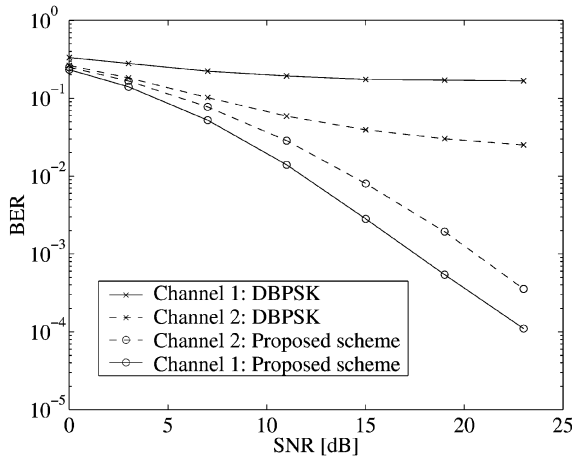


Fig. 3. Performance comparison between DBPSK and our proposed scheme for two different two-path channels. **Ch1**: $\mathbf{R}_h = \text{diag}\{[2/3 \ 1/3]\}$. **Ch2**: $\mathbf{R}_h = \text{diag}\{[1/1.05 \ 0.05/1.05]\}$. The block length is $N = 4$, and we have used $R = 1$ and $Q = 2$.

B. Comparison With Block Differential OFDM

In an OFDM context, standard differential encoding on each subcarrier yields poor performance due to loss of multipath diversity. However, the block differential encoding scheme proposed in [7], called block differential OFDM (B-DOFDM), preserves maximum diversity. This method divides the N subcarriers into M groups of length $L + 1$ in an optimal way, and encodes each block differentially, similar to (3), but with different generator matrices \mathbf{G}_m .

We will here compare our proposed method with B-DOFDM for a three-path channel ($L = 2$) with correlation matrix $\mathbf{R}_h = \mathbf{I}_3$. We assume that the original information symbols are BPSK symbols, and that $R = 1$. For the scheme proposed in this paper, we choose block length $N = K^2 = (L + 1)^2 = 9$. Hence, since $|\mathcal{A}_g| = 2^{RK} = 8$, the entries of \mathbf{g}_m in (7) are chosen from an 8-PSK constellation. For the B-DOFDM scheme, we use the same block length, and divide the nine subcarriers into three groups of $L + 1 = 3$ subcarriers. For both methods, we let the map $\mathcal{M}(\cdot)$ from information blocks to generator matrices be a Gray mapping to improve the coding gain.

The nonlinear effects introduced by the power amplifier will degrade the performance of a nonconstant modulus transmission. To demonstrate this effect, we introduce a clipping of the transmitted signal. Specifically, we define the input back-off (IBO) to be $\text{IBO} \triangleq NA^2/E\|\mathbf{u}\|^2 = A^2/E_s$, the ratio between the input power corresponding to a clipping at amplitude A and the signal power. For our transmission scheme, clipping has no direct effect on the critically sampled symbols, since these always have a constant amplitude less than the clipping level. For the B-DOFDM scheme, clipping results in a small loss of coding gain, and, more importantly, a BER saturation level.

Note that in practice, it is the continuous-time waveform entering the power amplifier that gets clipped. This waveform may have peaks between the symbol-rate samples used in the detection. Clipping of these peaks introduces some nonlinear effects, even in our scheme. However, simulation of this phenomenon is beyond the scope of this paper, and it is thus ignored, assuming

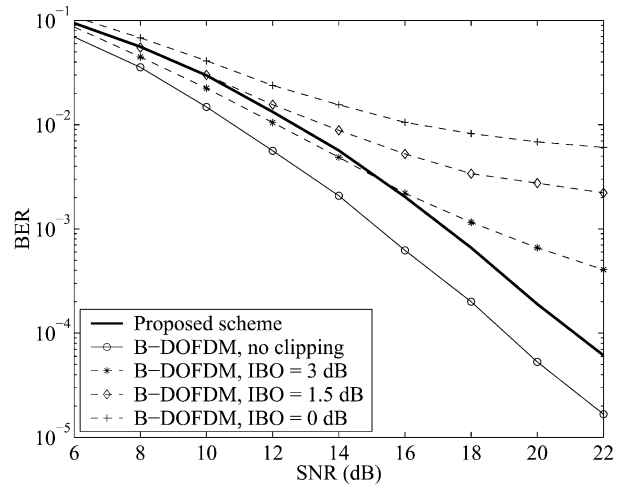


Fig. 4. Performance comparison between B-DOFDM and our proposed scheme for a three-path channel with autocorrelation matrix $\mathbf{R}_h = \mathbf{I}_3$, and block length $K = 9$. The performance of B-DOFDM is shown for several values of IBO, as well as the ideal, nonclipped case.

that this effect results in an equal degradation of the BER performance of all considered schemes. The results below should be interpreted with this in mind.

The simulation results are shown in Fig. 4. Both methods achieve full diversity without clipping. Consequently, the BER curves are parallel at high SNR. For $\text{BER} = 10^{-3}$, B-DOFDM has about 2 dB better performance. However, as mentioned earlier, clipping degrades the performance of B-DOFDM, while the scheme proposed in this paper is not affected. For $\text{BER} = 10^{-3}$, the constant modulus transmission scheme performs about 1 dB better than B-DOFDM with IBO = 3 dB. With even more clipping, the B-DOFDM technique never achieves $\text{BER} = 10^{-3}$ due to a high BER saturation level.

C. PAPR Reduction

Define the instantaneous PAPR by

$$\text{PAPR}[z] = \frac{\|\bar{\mathbf{u}}_{L_u}[z]\|_\infty^2}{E_s}$$

where $\bar{\mathbf{u}}_{L_u}[z]$ is an upsampled and filtered version of $\bar{\mathbf{u}}[z]$, and L_u is the upsampling factor. This is a much more accurate approximation of the continuous-time waveform than the symbol-rate sampled $\bar{\mathbf{u}}[z]$. The oversampling factor used here is $L_u = 8$, and the IFFT-based oversampling strategy is given in [12, p. 18]. This strategy corresponds to using sinc pulses, which, in practice, are not usable due to high out-of-band radiation. However, using more realistic shaping pulses, like a square-root raised cosine, will not alter the results below significantly. Hence, we will use the IFFT-based oversampling strategy for simplicity.

Fig. 5 shows estimates of $\Pr(\text{PAPR}[z] > \gamma)$, the PAPR outage probability, obtained by randomly selecting 100 000 input blocks and channels. For the conventional coded differential OFDM (CDOFDM) system, we use differential (D)QPSK ($Q = 4$) over each of the 48 subcarriers. On each side of the data block, we insert eight zero carriers as a guard band, such that the overall FFT size is $\tilde{N} = 64$. The information bits are

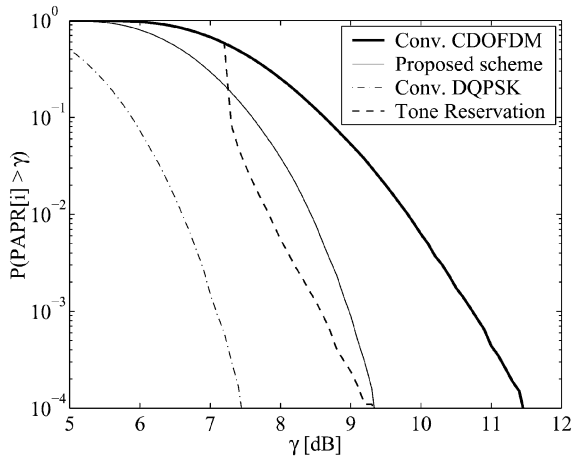


Fig. 5. PAPR outage probability of conventional differential OFDM (dashed) with block length $\tilde{N} = 48$, and the scheme proposed in this paper (solid) with $M = 3$ groups of $N = 16$ subcarriers, respectively. The transmission rate is 1 b/s/Hz for both systems.

coded by an optimal four-state trellis code [10, p. 492] with rate $R = 1/2$, yielding an overall rate of $R \log_2 Q = 1$. The coded bits are then mapped onto QPSK symbols and differentially modulated. The decoding complexity of this scheme is $O(4\tilde{N})$. For the proposed scheme, we apply the block differential encoding on $M = 3$ groups of $N = 16$ subcarriers, also with eight zero carriers on each side. The rate is $R \log_2 Q = 1$ as in the CDOFDM scheme, and the complexity is $O(\tilde{N})$, as seen in (9). We have also included the result of combining the CDOFDM scheme with the PAPR reduction scheme outlined in [12, p. 81], which is based on tone reservation. To keep the additional transmitter complexity of this iterative method reasonable, we limit the number of iterations (each of which is $O(\tilde{N})$) to five, the step size used is $\mu = 25$, the clip level is 6 dB, and we aim to cancel only the largest peak. The four reserved subcarriers are chosen by random optimization [12, p. 91] from the set $\{6, 7, \dots, 57\}$, that is, we have reduced the number of guards to six on each side of the information block, in order to maintain the same rate as for the proposed scheme. For completeness, the PAPR outage probability for a conventional single-carrier DQPSK transmission using sinc pulses is also shown.

Observe that we have achieved a gain relative to the conventional CDOFDM system of 1.5 dB at $\Pr(\text{PAPR}[i] > \gamma) = 10^{-2}$, and 2.5 dB at $\Pr(\text{PAPR}[i] > \gamma) = 10^{-3}$, respectively. The PAPR reduction achieved is comparable to the result achieved by tone reservation with a reasonable number of iterations.

Fig. 6 shows the corresponding results for a system with 128 subcarriers. The proposed scheme uses $M = 6$ groups of $N = 16$ subcarriers, and 16 zero carriers on each side, while the conventional CDOFDM uses 96 subcarriers, and 16 zero carriers on each side. The tone reservation scheme uses eight reserved subcarriers chosen from the set $\{12, 13, \dots, 115\}$ by random optimization, the step size is $\mu = 40$, the clip level is still 6 dB, and we use 12 zero carriers on each side.

Observe that with these parameters, the tone reservation scheme performs about 1 dB better for PAPR outage probab-

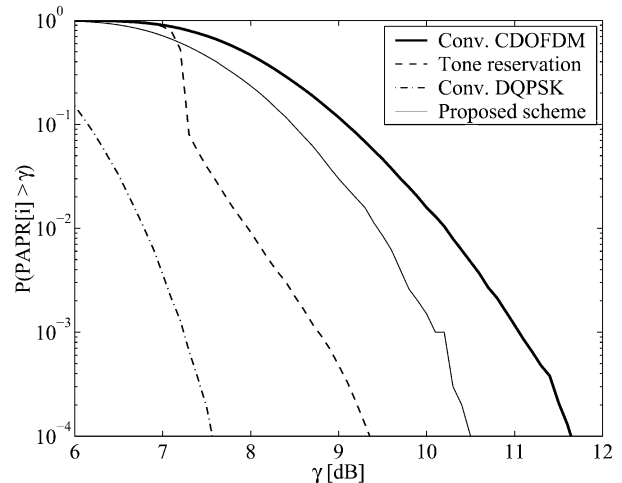


Fig. 6. PAPR outage probability of conventional differential OFDM (dashed) with block length $\tilde{N} = 48$, and the scheme proposed in this paper (solid) with $M = 3$ groups of $N = 16$ subcarriers, respectively. The transmission rate is 1 b/s/Hz for both systems.

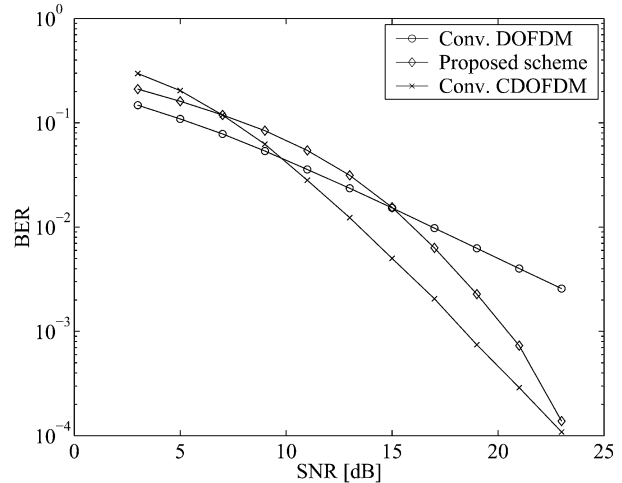


Fig. 7. Comparison of BER performance for the systems compared in Figs. 5 and 6.

ities smaller than 0.1, and that the PAPR gain of the proposed scheme is moderate.

Fig. 7 shows the BER performance of the systems used above for rate $R = 1$, as well as for an uncoded DOFDM with the same rate. The $L + 1 = 16$ channel taps are i.i.d. zero-mean complex Gaussian variables with variance $1/(L + 1)$. The proposed scheme provides a diversity order of $K = 4$, and thus has a performance comparable with the CDOFDM scheme. Notice that the tone reservation does not affect BER performance, since the reserved tones simply are discarded at the receiver.

D. Complex Field Coding

As mentioned in Section VII, using $\Theta \neq \mathbf{I}_K$ turns out to yield better BER performance only for low rates ($R < 1$). We demonstrate this by an example. Let the block length be $N = 16$, and the channel order be $L = 10$. Here, $K = 4 < L$, such that we do not enable maximum multipath diversity without extra complex field coding, i.e., with $\Theta = \mathbf{I}_K$. Assuming BPSK symbols ($Q = 2$), and defining Θ to be circulant with $[1 \ 16^{-R} \ 0 \ \dots \ 0]$ as its first row, we enable more diversity.

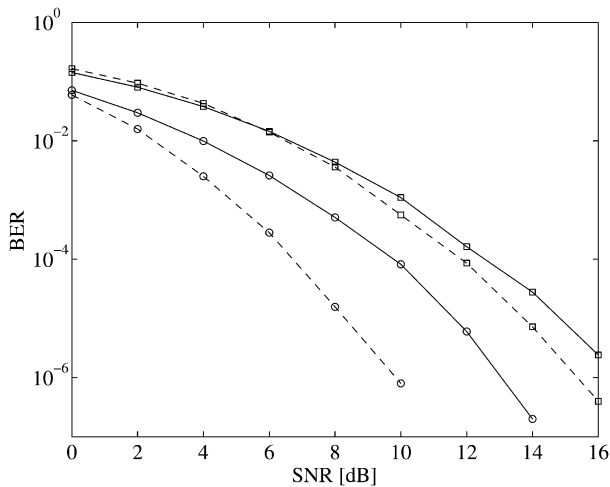


Fig. 8. BER curves for the complex-field-coded constant modulus scheme. Block length is $N = 16$, and the channel has order $L = 10$. For the solid lines, we have used $\Theta = \mathbf{I}_4$ with rate $R = 1/2$ (squares) and $R = 1/4$ (circles), respectively. The dashed lines are the corresponding results when we let Θ be circulant with $[1 \ 16^{-R} \ 0 \ 0]$ as its first row.

In Fig. 8, we show the BER performance with (dashed lines) and without (solid lines) extra complex field coding for rates $R = 1/2$ (squares) and $R = 1/4$ (circles), respectively. For rate $R = 1/2$, the extra diversity starts to show up at around 6 dB, yielding a 1-dB SNR gain at $\text{BER} = 10^{-4}$, which is not a lot, considering that we have sacrificed the linear decoding complexity of the simple scheme. For rate $R = 1/4$, however, the extra diversity shows up already at 0 dB, yielding a 3-dB SNR gain at $\text{BER} = 10^{-4}$.

Note that the cyclic prefix overhead in this case is rather large, which leads to a reduced spectral efficiency. However, this can be mitigated, without changing the BER performance, by relaxing the constant modulus requirement, as discussed in Section VI.

IX. CONCLUSIONS

We have in this paper designed a block differential encoding scheme that exploits the multipath diversity of a frequency-selective channel, and at the same time preserves the constant modulus property of the original time-domain symbols. Constant modulus transmitted symbols ensure that the PAPR of the transmitted waveform is reduced by a large factor, thus reducing the nonlinear effects of the power amplifier.

We have shown that the ML decoder for our system could be simplified to yield a decoder with complexity that increases only linearly with the block length. Extension to multiple-symbol differential detection, at the cost of increased complexity, is straightforward. Analysis of the PEP showed that our method preserves the multipath diversity. The coding gain, however, turned out to be a monotonically decreasing function of the block length, which means that the performance under moderate SNR conditions will degrade for large block lengths.

The scheme may be applied in practical OFDM systems by grouping the subcarriers into shorter subblocks, and applying the constant modulus scheme to each of the subblocks separately. This yields an upper bound on the PAPR of the

symbol-rate samples, which, in turn, leads to a reduction in the continuous-time PAPR.

In situations where we can sacrifice rate, additional complex field coding, linear in the phase domain, yields better performance by enabling more multipath diversity, provided that the channel is long enough that the simple constant modulus scheme does not already exploit all the diversity provided by the channel.

Numerical simulations indicated that the proposed constant modulus scheme significantly outperforms conventional DBPSK, even in nearly flat-fading channels, such as a channel with a small blind equalization error. The method was also compared with an existing B-DOFDM scheme, and found to have comparable performance in short channels, even when nonlinear effects are ignored. Due to the constant modulus property of the transmitted symbols, our method does not suffer much from nonlinear effects, and consequently has superior performance for high SNR when input clipping is introduced. For a moderate number of subcarriers, it was shown that the proposed subcarrier grouping scheme may improve diversity, and at the same time, has BER and PAPR characteristics similar to CDOFDM with tone reservation, with lower encoder and decoder complexity. For a larger number of subcarriers, the PAPR reduction is smaller, though this can be mitigated by increasing the subcarrier group size, thereby trading off rate or BER performance. Finally, we showed that additional complex field coding yields better performance when low rates are considered, at the expense of a higher decoding complexity.

ACKNOWLEDGMENT

Y. Larsen and G. Leus would like to thank G. B. Giannakis for the opportunity to visit the University of Minnesota during the academic year Fall 2001–Fall 2002, where this work was initiated. Y. Larsen also acknowledges important and interesting discussions with A.-B. Salberg during the finalization of this work.

REFERENCES

- [1] K. L. Baum and N. S. Nadgouda, "A comparison of differential and coherent reception for a coded OFDM system in a low C/I environment," in *Proc. GLOBECOM Conf.*, vol. 1, Phoenix, AZ, 1997, pp. 300–304.
- [2] D. C. Chu, "Polyphase codes with good periodic correlation properties," *IEEE Trans. Inform. Theory*, vol. IT-18, pp. 531–532, July 1972.
- [3] B. Daneshrad, L. J. Cimini, and M. Carloni, "Clustered-OFDM transmitter implementation," in *Proc. Int. Symp. Personal, Indoor and Mobile Radio Communications*, vol. 3, Taipei, Taiwan, Oct. 15–18, 1996, pp. 1064–1068.
- [4] D. Divsalar and M. K. Simon, "Multiple-symbol differential detection of MPSK," *IEEE Trans. Commun.*, vol. 38, pp. 300–308, Mar. 1990.
- [5] D. L. Goeckel and G. Ananthaswamy, "On the design of multidimensional signal sets for OFDM systems," *IEEE Trans. Commun.*, vol. 50, pp. 442–452, Mar. 2002.
- [6] Y. Larsen, G. Leus, and G. B. Giannakis, "Constant modulus block differential encoding for frequency-selective channels," presented at *Proc. Conf. Information Sciences and Systems*. [CD-ROM]
- [7] Z. Liu and G. B. Giannakis, "Block differentially encoded OFDM with maximum multipath diversity," *IEEE Trans. Wireless Commun.*, vol. 2, pp. 420–423, May 2003.
- [8] K. G. Paterson and V. Tarokh, "On the existence and construction of good codes with low peak-to-average power ratios," *IEEE Trans. Inform. Theory*, vol. 46, pp. 1974–1987, Sept. 2000.

- [9] B. M. Popović, "Generalized chirp-like polyphase sequences with optimum correlation properties," *IEEE Trans. Inform. Theory*, vol. 38, pp. 1406–1409, July 1992.
- [10] J. Proakis, *Digital Communications*, 4th ed. New York: McGraw-Hill, 2001.
- [11] V. Tarokh, N. Seshandri, and A. R. Calderbank, "Space–time codes for high-data-rate wireless communication: Performance criterion and code construction," *IEEE Trans. Inform. Theory*, vol. 44, pp. 744–765, Mar. 1998.
- [12] J. Tellado, *Multicarrier Modulation With Low PAR—Applications to DSL and Wireless*. Norwell, MA: Kluwer, 2000.
- [13] Z. Wang and G. B. Giannakis, "Wireless multicarrier communications: Where Fourier meets Shannon," *IEEE Signal Processing Mag.*, vol. 19, pp. 29–48, May 2000.
- [14] ———, "Complex-field coding for OFDM over fading wireless channels," *IEEE Trans. Inform. Theory*, vol. 49, pp. 707–720, Mar. 2003.
- [15] Z. Wang, X. Ma, and G. B. Giannakis, "OFDM or single-carrier zero-padded block transmissions?," *IEEE Trans. Commun.*, vol. 52, pp. 380–394, Mar. 2004.



Yngvar Larsen (A'04) was born in Tromsø, Norway, in 1976. He received the Diploma in applied physics and the Ph.D. degree in physics from the University of Tromsø, Tromsø, Norway, in 1999 and 2003, respectively.

He was a Research Scholar with the Department of Physics, University of Tromsø, from January 2000 to December 2003. Currently, he is with NORUT Information Technology Ltd., Tromsø, Norway. During the summer of 1999, he was a Summer Research Assistant with the NATO SACLANT

Undersea Research Centre, La Spezia, Italy, and from July 2001 to June 2002 he was a Visiting Researcher with the University of Minnesota, Minneapolis. His research interests are in the area of statistical signal and array processing and communications.



Geert Leus (M'01) was born in Leuven, Belgium, in 1973. He received the electrical engineering degree and the Ph.D. degree in applied sciences from the Katholieke Universiteit Leuven, Leuven, Belgium, in 1996 and 2000, respectively.

He was a Research Assistant and a Postdoctoral Fellow of the Fund for Scientific Research—Flanders, Belgium, from October 1996 till September 2003. During that period, he was affiliated with the Electrical Engineering Department of the Katholieke Universiteit Leuven, Belgium. Currently, he is an

Assistant Professor at the Faculty of Electrical Engineering, Mathematics and Computer Science, Delft University of Technology, Delft, The Netherlands. During the summer of 1998, he visited Stanford University, Stanford, CA, and from March 2001 till May 2002 he was a Visiting Researcher and Lecturer at the University of Minnesota, Minneapolis. His research interests are in the area of signal processing for communications.

Dr. Leus received a 2002 IEEE Signal Processing Society Young Author Best Paper Award. He is a member of the IEEE Signal Processing for Communications Technical Committee, and an Associate Editor for the *IEEE TRANSACTIONS ON WIRELESS COMMUNICATIONS* and the *IEEE SIGNAL PROCESSING LETTERS*.



Georgios B. Giannakis (S'84–M'86–SM'91–F'97) received the Diploma in electrical engineering from the National Technical University of Athens, Greece, in 1981. He received the M.Sc. degree in electrical engineering in 1983, M.Sc. degree in mathematics in 1986, and the Ph.D. degree in electrical engineering in 1986, from the University of Southern California (USC), Los Angeles.

After lecturing for one year at USC, he joined the University of Virginia, Charlottesville, in 1987, where he became a Professor of Electrical Engineering in 1997. Since 1999, he has been with the University of Minnesota, Minneapolis, as a Professor in the Department of Electrical and Computer Engineering, and holds an ADC Chair in Wireless Telecommunications. His general interests span the areas of communications and signal processing, estimation and detection theory, time-series analysis, and system identification, subjects on which he has published more than 180 journal papers, 340 conference papers, and two edited books. Current research focuses on transmitter and receiver diversity techniques for single- and multiuser fading communication channels, complex-field and space–time coding, multicarrier, ultra-wideband wireless communication systems, cross-layer designs, and distributed sensor networks.

Dr. Giannakis is the corecipient of five Best Paper Awards from the IEEE Signal Processing (SP) Society (1992, 1998, 2000, 2001, and 2003). He also received the Society's Technical Achievement Award in 2000. He co-organized three IEEE-SP Workshops, and guest co-edited four special issues. He has served as Editor in Chief for the *IEEE SIGNAL PROCESSING LETTERS*, as Associate Editor for the *IEEE TRANSACTIONS ON SIGNAL PROCESSING* and the *IEEE SIGNAL PROCESSING LETTERS*, as secretary of the SP Conference Board, as member of the SP Publications Board, as member and vice-chair of the Statistical Signal and Array Processing Technical Committee, and as chair of the SP for Communications Technical Committee. He is a member of the Editorial Board for the *PROCEEDINGS OF THE IEEE*, and the steering committee of the *IEEE TRANSACTIONS ON WIRELESS COMMUNICATIONS*. He is a member of the IEEE Fellows Election Committee, and the IEEE-SP Society's Board of Governors.